NAWMS: Nonintrusive Autonomous Water Monitoring System

Younghun Kim, Thomas Schmid, Zainul M. Charbiwala,
Jonathan Friedman, Mani B. Srivastava

Networked and Embedded Systems Lab.
Electrical Engineering Department
University of California, Los Angeles, CA 90095, USA
{kimyh,thomas.schmid,zainul,jf,mbs}@ucla.edu

ABSTRACT

Water is nature's most precious resource and growing demand is pushing fresh water supplies to the brink of non-renewability. New technological and social initiatives that enhance conservation and reduce waste are needed. Providing consumers with fine-grained real-time information has yielded benefits in conservation of power and gasoline. Extending this philosophy to water conservation, we introduce a novel water monitoring system, NAWMS, that similarly empowers users.

The goal of our work is to furnish users with an easy-to-install self-calibrating system that provides information on when, where, and how much water they are using. The system uses wireless vibration sensors attached to pipes and, thus, neither plumbing nor special expertise is necessary for its installation. By implementing a non-intrusive, autonomous, and adaptive system using commodity hardware, we believe it is cost-effective and widely deployable.

NAWMS makes use of the existing household water flow meter, which is considered accurate, but lacks spatial granularity, and adds vibration sensors on individual water pipes to estimate the water flow to each individual outlet. Compensating for manufacturing, installation, and material variabilities requires calibration of these low cost sensors to achieve a reasonable level of accuracy. We have devised an adaptive auto-calibration procedure, which attempts to solve a two phase linear programming and mixed linear geometric programming problem.

We show through experiments on a three pipe testbed that such a system is indeed feasible and adapts well to minimize error in the water usage estimate. We report an accuracy, over likely domestic flow-rate scenarios, with long-term stability and a mean absolute error of 7%.

Categories and Subject Descriptors

H.4 [**Information Systems Applications**]: Miscellaneous

General Terms

Algorithms, Design, Experimentation, Human Factors, Measurement, Performance, Theory

Keywords

Adaptive Sensor Calibration, Machine Learning, Water Flow Rate Estimation, Nonintrusive and Spatially Distributed Sensing, Tiered Information Architecture, Parameter Estimation via Optimization

1. INTRODUCTION

Bob hears about water conservation all the time. He is told that if every citizen consumed water moderately, our supplies would last forever. But, what is moderate? Is he wasting water? He decides to consult his utility bill, but quickly realizes that the monthly usage is for the *whole house.* What he needs is a system that can tell him not just how much water is being used, but where it gets used, when, and by whom. Having a system prompt him in real-time about usage for every outlet in the house puts him in a better position to discover wastage and make corrections.

The problem Bob faces applies to any resource a household consumes. Most utilities do not provide the spatial and temporal granularity needed for household members to effectively reduce their resource consumption, since it would mean higher installation and infrastructure cost. The systems currently in place are adequate for their billing purposes.

McMakin [28], Ester [18] and Stern [38] show in their studies that providing fine-grained consumption information helps consumers pinpoint waste, and enables improved efficiency. They also show that consumers are motivated to conserve, "do the right thing", and reduce expenses. At a macroscopic level, conservation improves a country's overall resource management. For example, the U.S. Environmental Protection Agency claims that 3 trillion gallons of water could be saved each year if every household in the U.S. decreased its water consumption by 30 percent [41]. This results in a dollar-volume saving of $49.3 million per day, or more than *$18 billion a year*! Water conservation is of even greater financial significance as increasing purification cost

is being compounded by rapid demand growth. American public water supply and treatment facilities consume about 56 billion kWh per year – enough electricity to power over 5 million homes [41]. To make things worse, higher global temperatures are affecting our fresh water reserves in ice and snow caps. The Water Poverty Index [10] illustrates that an urgent global initiative toward conservation is necessary.

The first step toward conservation is measurement [18, 28, 38]. For electricity, small power monitoring sensors have emerged [15], but they are too expensive to be installed on every electric appliance. For water, there is nothing analogous available. Current consumer-grade water flow meters are meant to be installed inline, requiring non-trivial plumbing, best handled by a professional. Thus, conventional means of deriving high resolution data would come with high installation cost. In some cases, where spatially dense water monitoring systems are essential for correct operation, this is justifiable (e.g. irrigation systems [9] or pharmaceutical manufacturing plants).

The challenge is designing a system that provides the same resolution at a cost and effort that is reasonable for household use. To this end, we propose NAWMS: a scalable water monitoring system capable of estimating water flow rate using wireless sensor network technology. NAWMS uses inexpensive vibration sensors attached externally to pipes. This reduces both cost and effort of installation. Inexpensive sensors and their un-controlled installation, however, introduce noise and variability in the measurements. NAWMS uses a novel feedback optimization formulation that continuously recalibrates the sensors, thus minimizing the estimation error for the total water consumption.

The contribution of this paper is three fold:

Well Defined Tiered Information Architecture:
> We introduce a well defined tiered information architecture. The first tier is accurate but spatially coarse grained. The second tier is less accurate but spatially fine grained. We exploit the two-tiered information architecture to achieve spatially fine grained and accurate results(Fig. 1).

Realistic Modeling of a Water Monitoring System:

> A sensor system needs to capture realistic constraints such as external noise, physical limitations and characteristics, and performance requirements. Our model takes these into account in order to compensate for side-effects.

Autonomous and Adaptive Calibration:
> A sensor system often suffers from complex calibration, and its periodic recalibration increases maintenance cost. A well defined performance metric that evaluates the system on the fly, and an optimization problem formulation that yields calibration parameters, enable the system to autonomously and adaptively calibrate the water monitoring system while regulating its performance.

The rest of the paper is structured as follows. Section 2 presents related work. We continue by describing the conceptual system architecture of NAWMS in Section 3. In Section 4 we formulate the mathematical challenges and introduce several optimization problems to solve them. Our

system evaluation can be found in Section 6, where we describe our prototype and present the achieved system performance. Finally, Section 7 contains future work for NAWMS.

2. RELATED WORK

There are two broad classes of related work: (a) Infrastructure monitoring for activity classification and maintenance, and (b) water flow rate measurement techniques.

Infrastructure provides useful behavioral information about its inhabitants and often times this information can be extracted through simple interfaces and means. For example, Patel [31] monitors the electrical noise within the powerlines of a house. They exploit the fact that each appliance introduces a unique noise signature. By detecting and identifying this signature, they can infer if an appliance is on or off but not its actual power consumption. Fogarty [21] investigated monitoring of the plumbing system by using microphones on pipes to infer water activity in a household. Both systems are easy to install but employ complex calibration mechanisms in order to learn the detection patterns. Though these systems capture user behavior, we consider them incomplete for conservation because they do not estimate actual consumption numbers.

At a larger scale, cities are struggling with the maintenance of aging water distribution and treatment systems. Stoianov [39] describes an interesting prototype sensor network that can monitor different water characteristics in real-time. In a lab setup, they demonstrated how one can detect a water leak in a pipe, by analyzing the frequency spectrum of an accelerometer. Even though they use similar hardware, Stoianov's system has a completely different goal and uses a different mathematical approach.

Methods to measure the water flow rate, or more generally the flow of liquid in pipes, is of great interest to many fields. For example, chemical processes often require precise control over fluid flow [37], agricultural irrigation networks need monitoring to avoid over-watering [36], and utility companies deploy inline water flow meters for billing purposes. The methods could be divided into two categories: (a) open channel water monitoring/discharged water monitoring and (b) water flow rate estimation in closed pipes.

Large scale irrigation systems generally use open channels to distribute water to different areas. Trimmer [40] describes a way to estimate the discharged water flow rate by observing the water level and pipe diameter. Bankston [3] provides look-up tables that map manually obtained observations to the flow rate of an open channel. Unfortunately, this method is laborious and lacks real-time response.

Modern irrigation networks leverage wireless sensor network technology to monitor the water flow rate in each water channel. Additionally, they use this information to regulate the flow rate in real-time. These distributed irrigation control systems are a showcase for wireless sensors and actuators that deliver optimal water volume for agricultural irrigation [9].

Measuring the flow rate of a liquid in a closed pipe is further divided into two categories: inline direct flow measurement and non-intrusive flow estimation. The most common example of inline flow measurement is the main water flow meter in a household that utility companies install. These meters use a mechanical turbine that spins at an angular velocity proportional to water flow rate. The constant of proportionality is the exact diameter of the flow chamber,
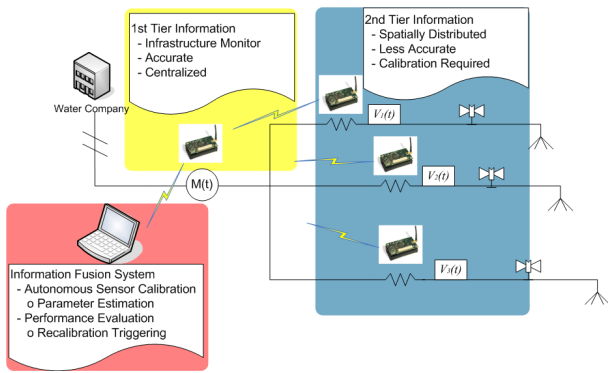
Figure 1: NAWMS system and information architecture

which is estimated though factory calibration. Thus, counting the number of rotations of the turbine yields directly the flow rate in the pipe. The disadvantage of this technique is that it needs to be installed between pipes segments, requiring plumbing expertise. This is feasible during initial construction, but retrofitting pipes is tedious and expensive.

Several techniques for a non-intrusive flow rate estimation exist. The most common one uses ultrasound [19]. This technique is based on an ultrasound transmitter and receiver pair that either measures the induced doppler shift in the received signal, or the transmission time within the liquid medium. Unfortunately, commercially available devices [16] cost over $1000 a unit and require delicate installation. Thus, they are reserved for industrial, or diagnostic testing purposes.

An innovative technique described by Evans [20] exploits the vibration induced by the flow of liquid in pipes. This technique is potentially cost-effective, since it uses an accelerometer, and the data processing is trivial. However, it requires careful calibration because the vibrations depend heavily on the pipe material used and the sensor-to-pipe attachment.

NAWMS combines the pre-installed inline flow meter (first information tier) with non-intrusive inexpensive vibration based sensors (second information tier) in order to provide an accurate per pipe flow rate. NAWMS exploits the high accuracy of the first information tier to autonomously calibrate the less precise, though spatially finer grained, second information tier.

3. NAWMS SYSTEM ARCHITECTURE

A sensor usually measures a physical phenomenon indirectly. For example, a temperature sensor exploits thermal variation of resistance, a light sensor measures photo conductivity, etc. Due to this indirectness, a sensor needs calibration to establish a mathematical mapping between sensor readings and the physical phenomena. Some sensors can be bought factory calibrated, and some don't even need calibration. One example is the inline water flow meter. Since its package dimensions are known during fabrication, there is a well defined relation between turbine speed and flow rate. Unfortunately, it is infeasible to retrofit a household or an entire building with these sensors. For this reason, we need a system that indirectly measures water flow within a pipe.

3.1 Tiered Information Architecture

We propose NAWMS, a two tiered information architecture that consists of one accurate pre-calibrated sensor that provides us with the sum of all flows and an uncalibrated vibration sensor for each individual pipe (Fig. 1). This architecture has three characteristics:

- The first tier is reliable, and the service provider maintains it. A user does not have to worry about its accuracy or correct operation.

- The calibration of the non-intrusive vibration based water flow sensors can be automated considering the correlation between the first and second tier information sources.

- The first tier is 'ground truth' that is always available. This allows the system to compute and adapt the calibration parameters continuously.

3.2 Hardware and Software Architecture

The system consists of three main hardware and software components with the following associated challenges:

- *Tapping Into Existing Infrastructure:* The main water meter provides accurate water flow rate for the entire household. However, a mechanism is needed to extract readings with high fidelity for the NAWMS system.

- *Spatially Distributed Vibration Based Water Flow Rate Sensors:* Accelerometers measure the vibrations according to the microscopic water flow model in a pipe. These accelerometers need to be calibrated in order to achieve a good estimate.

- *Information Fusion Algorithm:* Calibration requires a lot of time and human intervention. In this paper we propose several optimization formulations that enable the system to calibrate its parameters and coefficients automatically using an open source optimization toolbox.

3.2.1 Tapping Into Existing Infrastructure

There are several commercially available products [1, 2, 25] that allow one to interrogate the main water meter in real-time. Various types of "pulsers" [25] provide a pulse train that is proportional to the water flow rate in the pipe. A microcontroller based circuit, such as a "sensor mote" utilizing its built-in interrupts and timers, can easily decode such a signal providing real-time water flow information.

Another approach was described by Chueng [12]. His technique uses a hall effect sensor that picks up a varying magnetic field produced by the spinning collector unit. He reports volume measurements with a resolution of 0.005 gallon.

Fortunately, a better solution is expected in the near future. The Automatic Meter Reading Association [2] and the American Water Works Association [1] are developing a system that relays real-time meter information wirelessly for billing purposes. Two products, one from Germany [17], and another from the UK [35] are already available. Following the trend of utility companies simplifying their billing systems through wireless technologies, we believe that extracting data from the main water meter of a household in real-time will soon be commonplace.
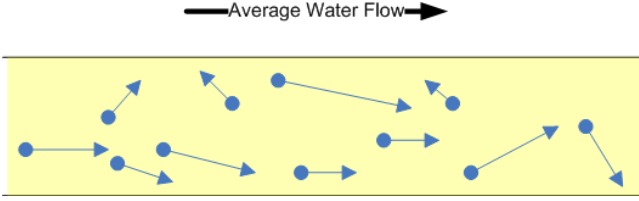
Figure 2: Microscopic view of the water flow in a pipe.

3.2.2 Non-intrusive Water Flow Rate Measurement Using Vibration Sensors

As Evans described in [20], the flow rate in a pipe is proportional to the vibration of a pipe. We describe this effect in further detail in Section 4.1. A sensor network node equipped with a one dimensional accelerometer is adequate to capture this signal since variance in the measured acceleration is a measure of vibration. Estimating variance is computationally simple, and thus can be done locally. This results in low communication load. We describe other details of the prototype used in Section 6.

3.2.3 Information Fusion, Optimization Toolbox, and Aggregation Unit

The data collected by the vibration sensors is sent to the fusion center, where the samples and the reading from the main meter are "fused" to solve the mathematical optimization problems introduced in Section 4.2. The solution calculates the calibration parameters for the individual vibration sensors, which can then be used to map to real-time flow in each pipe.

Many ready-to-use optimization problem solvers exist. In our implementation, we use the CVX toolbox [8,14], an open source convex optimization tool. Other advanced tools, such as MOSEK [29], could also be used.

4. PROBLEM DESCRIPTION AND FORMULATION

This section is further decomposed into the underlying pipe dynamic theories, their application to household plumbing, and the resulting formal optimization problem statements.

4.1 Water Flow Rate Estimation using Vibration Sensors

4.1.1 Theory of Operation

To understand how flow rate and vibration in a pipe are related, we cover the basics of its micro-model. Water molecules on average all travel in the main direction of flow, as depicted in Figure 2. However, many molecules collide against the pipe wall. According to the first law of thermodynamics, some part of this kinetic energy converts to heat as the turbulent eddies dissipate, but most of it translates into potential energy in the form of pressure [32]. The pipe, in turn, deforms converting potential to kinetic (during deformation) and back to potential as deformation completes. The elasticity of the pipe material applies a restoring force. Evans shows [20] that vibration in a pipe results from this energy conversion cycle and is proportional to the average flow rate within the pipe.
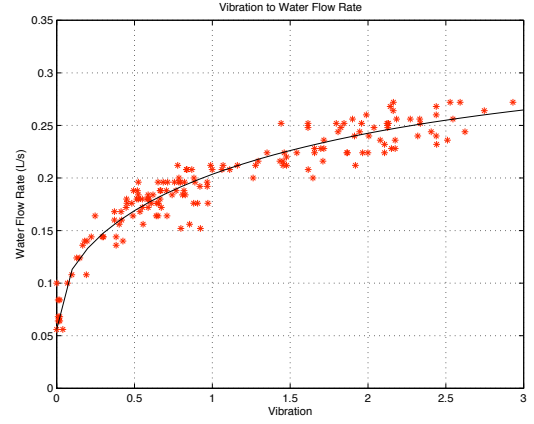

Figure 3: Measured pipe vibration for different flow rates for a 3/4" copper pipe.

The main result of Evan's work is based on the fact that the velocity of a fluid at a point in the pipe can be decomposed into the time average velocity$(\bar{u}, \bar{v})$ and fluctuating velocity(u', v'). Although there is no net flow in the perpendicular direction to the pipe axis, the time averaged velocity in that direction $\bar{v}$ is zero, the time average of their product $u' \cdot v'$ are, in general, negative.

From a non-trivial derivation by Evan et. al., we see

$$\frac{\partial^2 y}{\partial t^2} = -CEI\frac{\partial^4 y}{\partial x^4} = -Cp'(x) \qquad (1)$$

where,
$C = \frac{g}{A\gamma}$
A : cross sectional area of the beam
γ : specific weight of the beam
g : gravity
EI : flexural rigidity.

This essentially indicates that the transverse acceleration of the pipe is proportional to the pressure fluctuations in the fluid.

The principle of operation is based on the relationship between the standard deviation of the pipe vibration and the mean flow rate of the fluid in the pipe. Blake stated in [5] that the generation of vibration by fluid motion involves the reaction of fluids and solids to stresses imposed by time-varying flow. For dynamically similar flows, the ratio of the flow fluctuations to the average flow is constant. Bird shows [4] this relationship by noting that the oscillatory term is the time average of the absolute magnitude of the oscillation, given by $\sqrt{\bar{m}}$ where $m = u'^2$. They define this as "intensity of turbulence", which is a measure of the magnitude of the turbulent disturbance, and is given by $\frac{\sqrt{\bar{m}}}{\bar{u}}$.

From the definition of turbulent flow, the intensity of turbulence expression is rearranged as

$$\frac{\bar{m}}{\bar{u}^2} = \frac{\frac{1}{N}\sum_{i=1}^{N}[u_i(t) - \bar{u}]^2}{\bar{u}^2} \qquad (2)$$

where,
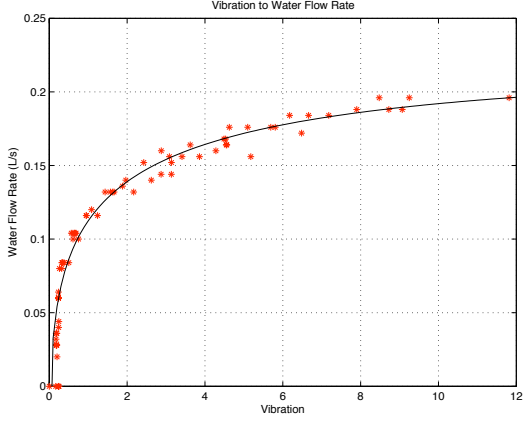$\bar{u}$: average velocity
u: instantaneous velocity.

Figure 4: Measured pipe vibration for different flow rates for a 3/4" PVC pipe.

Multiplying both side by the number of points N and $\bar{u}^2$, and dividing by $N-1$, we get

$$\frac{1}{N-1}\sum_{i=1}^{N}[u_i(t)-\bar{u}]^2 = \frac{NC}{N-1}\bar{u}^2 = K\bar{u}^2 \qquad (3)$$

This shows that the flow fluctuations are proportional to the pressure fluctuations and the pressure fluctuations are proportional to the pipe vibration. It follows that the standard deviation of the pipe vibration is proportional to the average flow rate. This result does not necessarily imply that the water flow rate in a pipe is linearly proportional to the vibration of the pipe. Instead, it implies that it has a non-linear but proportional relation due to the non-linear characteristics of vibration sensors, pipe structure, turbulence, etc.

The end result eq. 3 gives an important point that regardless of the pipe mounting methods, shape, and topology, at any exposed point on a pipe we can find a signal that is strongly correlated with the water flow rate at that point.

4.1.2   Vibration to Flow Rate Model

To verify the theory explained in Section 4.1.1 we conducted a simple experiment. We attached accelerometers on two different pipes, a copper and a PVC pipe. We measured the vibration occurring on the pipes while changing the flow rate of the water running through it. Figure 3 and 4 illustrate the result. To find a mathematical relationship between vibration and flow rate, we tested the applicability of various models, details of which we cover in Section 6.1.1. We found that a third order root function,

$$f(t) = \alpha\sqrt[3]{v(t)} + \beta\sqrt{v(t)} + \gamma v(t) + \delta, \qquad (4)$$

where $f(t)$ is the water flow rate, and $v(t)$ the measured vibration, fit the measured data well. We use this function henceforth to map the measured vibration to the actual water flow rate in the pipe.

4.2   Simple Pipe Structure

In this section, we formulate the large scale water flow rate monitoring system for the pipe topology depicted in Figure 5. The system consists of the main water meter,
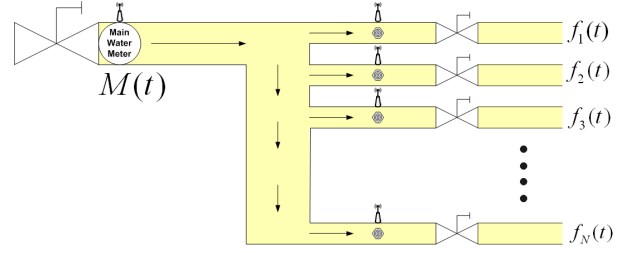

Figure 5: Simple pipe topology where one main pipe with flow rate $M(t)$ splits up into N subpipes.

and one vibration sensor on each of the N sub-pipes. The water meter provides the system with the real-time water flow $M(t)$, an accurate measurement for the main pipe. We denote the flow rate in each sub-pipe i, $f_i(t)$. Since all the sub-pipes are connected to the main pipe (assuming no leaks in the system), we have

$$M(t) = \sum_{i=1}^{N} f_i(t). \qquad (5)$$

where, $f_i(t) = \alpha_i\sqrt[3]{v_i(t)} + \beta_i\sqrt{v_i(t)} + \gamma_i v_i(t) + \delta_i$ as defined in the last section.

The goal of the calibration is to find the calibration parameters $\alpha_i, \beta_i, \gamma_i$ and δ_i for each sub-pipe. One possibility would be to attach a flow meter to each sub-pipe and calibrate each pipe individually. But this is tedious and involves manual effort. A better way is formulating a mathematical optimization problem that estimates these parameters simultaneously.

Assume that the sensors are synchronized, and that they sample the vibration every Δt seconds. Thus, Equation 5 in discrete-time becomes $M(k\Delta t) = \sum_{i=1}^{N} f_i(k\Delta t)$. After collecting K samples of $M(t)$ every Δt second, we get K equalities

$$M(k\Delta t) = \sum_{i=1}^{N} f_i(k\Delta t) \text{ for } k = 1,2,3,...,K. \qquad (6)$$

We define

$$\mathbf{M} \stackrel{def}{=} [M(\Delta t), M(2\Delta t), ..., M(K\Delta t)]^T$$

$$\mathbf{F} \stackrel{def}{=} \left[\sum_{i=1}^{N} f_i(\Delta t), \sum_{i=1}^{N} f_i(2\Delta t), ..., \sum_{i=1}^{N} f_i(K\Delta t)\right]^T.$$

We now formulate Equation 6 as an optimization problem because $\mathbf{M} = \mathbf{F}$ holds true, unless there is water leakage. Thus, the optimization problem is written as

$$\begin{aligned} \min \quad & ||\mathbf{M} - \mathbf{F}||_1 \\ \text{subject to} \quad & 0 \le f_i(k\Delta t) \le f_{i,max}. \end{aligned} \qquad (7)$$

Note that $M(k\Delta t)$ and $v_i(k\Delta t)$ are measurements from the sensors, and $\alpha_i, \beta_i, \gamma_i$ and δ_i are the decision variables. Additionally, the problem consists of linear constraints only, and its objective function is also be expressed as a linear function [6]. Therefore, any available Linear Programming solver can solve this problem very efficiently, and it guarantees a global optimum.
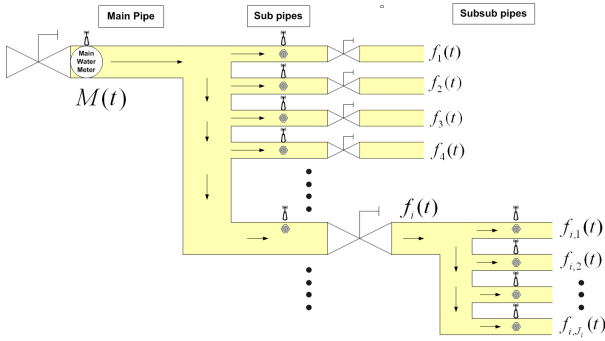
Figure 6: More realistic pipe topology where sub pipes can split up into sub-sub pipes.

The solution to the problem yields the calibration parameters for each individual pipe. Thus, no human intervention is necessary in order to calibrate the system, since everything is be automated.

4.3 General Pipe Structure

The plumbing system in a typical household is far more complicated than the simplified structure assumed in the previous section. We show in this section how even a complex structure can be reduced into several optimization problems, and that each of these problems is similar to Equation 7. This allows us to focus on the simple structure thereafter without loss of generality.

Consider the pipe structure depicted in Figure 6. Assuming no leakage, the total flow rate $M(t)$ is equal to the sum of the flow rates of each sub pipe. Similarly, the flow rate of each sub pipe is to the sum of the flow rate of its sub-sub pipes. Thus, from the law of mass conservation, we get the following equalities:

$$
\begin{aligned}
f_i(t) &= \sum_{j=1}^{J_i} f_{i,j}(t) \\
M(t) &= \sum_{i=1}^{N} f_i(t),
\end{aligned}
\tag{8}
$$

where, $f_{i,j}$ is the flow of sub-sub pipe j of sub pipe i and J_i is the number of sub-sub pipes of sub pipe i. Similar to $f_i(t)$, we define $f_{i,j}(t) \stackrel{def}{=} \alpha_{i,j} \sqrt[3]{v_{i,j}(t)} + \beta_{i,j} \sqrt{v_{i,j}(t)} + \gamma_{i,j} v_{i,j}(t) + \delta_{i,j}$. With these equations, we formulate a new optimization problem similar to Equation 7:

$$
\begin{aligned}
\min \quad & ||\mathbf{M} - \mathbf{F}||_1 \\
\text{subject to} \quad & 0 \le f_i(k\Delta t) \le f_{i,max}
\end{aligned}
\tag{9}
$$

where

$$
f_i(k\Delta t) = \begin{cases} \sum_{j=1}^{J_i} f_{i,j}(k\Delta t) & \text{if i-th sub pipe has} \\ & \text{sub-sub pipes} \\ f_i(k\Delta t) & \text{else} \end{cases}
$$

In general, the water flow rate in a pipe is the sum of the water flow rate in its sub pipes. Therefore, any tree like pipe structure can be formulated in a form similar to Equation 9.

4.4 Accounting for Vibration Propagation

We have assumed thus far that the vibration of a pipe does not affect other pipes. However, since pipes are physically coupled, vibration propagates to other pipe segments. This phenomenon needs to be accounted for in our equations. Vibration propagation depends on pipe topology, pipe material, interconnects, and flow rate. Nevertheless, the induced vibrations are relatively small. As a first order approximation, we assume that propagated vibration is linearly proportional to inherent vibration. This assumption is reinforced by actual experiments on our testbed, which are described in Section 6.1.1.

Consider vibration only in pipe j. We define the vibration propagation from pipe j to pipe i as:

$$
\tilde{v}_i(t) = p_{i,j} v_j(t)
\tag{10}
$$

where,
$\tilde{v}_i(t)$: Measured vibration on pipe i
$p_{i,j}$: Vibration propagation constant from pipe j to pipe i

$v_j(t)$: Water flow induced vibration on pipe j

Generalizing this to the case where the measured vibration on a pipe i is the superposition of all possible vibrations, we get

$$
\tilde{v}_i(t) = \sum_{j=1}^{N} p_{i,j} v_j(t)
$$

$$
\begin{aligned}
p_{i,j} = 1 & \quad \text{if } i = j \\
0 \le p_{i,j} < 1 & \quad \text{else}
\end{aligned}
$$

We now update our optimization problem to include the vibration propagation coefficients:

$$
\begin{aligned}
\min \quad & ||\mathbf{M} - \mathbf{F}||_1 \\
\text{subject to} \quad & 0 \le f_i(k\Delta t) \le f_{i,max} \\
& \tilde{v}_i(k\Delta t) = \sum_{j=1}^{N} p_{i,j} v_j(k\Delta t)
\end{aligned}
\tag{11}
$$

Introducing propagation coefficients adds a posynomial equality constraint to Equation 7. This renders the optimization problem non-linear and non-convex and harder to solve. In the following sections, we explore two ways of reformulating the problem as (a) a generalized geometric programming (GP) problem, by relaxing and restricting the constraints with reasonably tight bounds, while conserving physically meaningful values, and (b) a two phase linear programming (LP) problem by decomposing the optimization problem in two parts. It is well known that both, GP, and two phase LP problems can be solved in polynomial time [7, 8]. Either of the techniques can estimate the calibration parameters. Depending on system performance requirements, an algorithm could potentially select which one to use.

4.5 Mixed Linear Geometric Programming Model

The posynomial equality constraints due to vibration propagation coefficients prevent us from solving the optimization problem as a GP problem [7, 8]. Additionally, the objective

function is not in standard GP form. We require to reformulate it since this class of problems, called Signomial Programs, are in general NP-hard [13].

First, we introduce a slack vector $\mathbf{s} \overset{def}{=} [s_1, ..., s_K]^T \in \mathbb{R}_+^K$. We then reformulate Equation 11 using the slack vector to the equivalent problem:

$$
\begin{aligned}
\min \quad & \sum_{k=1}^{K} s_k \\
\text{subject to} \quad & -\mathbf{s} \le \mathbf{F} - \mathbf{M} \le \mathbf{s} \qquad (12)\\
& 0 \le f_i(k\Delta t) \le f_{i,max} \\
& \tilde{v}_i(k\Delta t) = \sum_{j=1}^{N} p_{i,j} v_j(k\Delta t) \qquad (13)
\end{aligned}
$$

By restricting the first constraint to be positive, we can rewrite equation 13 as

$$
\begin{aligned}
\min \quad & \sum_{k=1}^{K} s_k \\
\text{subject to} \quad & 0 \le \mathbf{F} - \mathbf{M} \le \mathbf{s} \\
& 0 \le f_i(k\Delta t) \le f_{i,max} \\
& \tilde{v}_i(k\Delta t) = \sum_{j=1}^{N} p_{i,j} v_j(k\Delta t) \qquad (14)
\end{aligned}
$$

This restriction shrinks the search space considerably, but could make the problem infeasible. In most of the cases, however, the problem is still solvable [13]. According to [13], relaxing the posynomial equality constraints with reasonable tightness allows us to reformulate the problem in standard GP form.

We assume the following relaxation, since measured vibration on a pipe is the sum of all propagated vibrations plus the vibration induced by the water flowing through that pipe. Thus,

$$
\sum_{j=1}^{N} p_{i,j} v_j(t) \le \tilde{v}_i(t) \quad \forall i \qquad (15)
$$

As a consequence, we can rewrite Equation 14 as

$$
\begin{aligned}
\min \quad & \sum_{k=1}^{K} s_k \\
\text{subject to} \quad & \mathbf{F} \le \mathbf{s} + \mathbf{M} \\
& 0 \le f_i(k\Delta t) \le f_{i,max} \\
& \sum_{j=1}^{N} p_{i,j} v_j(k\Delta t) \le \tilde{v}_i(k\Delta t). \qquad (16)
\end{aligned}
$$

According to [8] Section 7.3, this is a mixed linear GP problem, as its objective function is linear and all constraints are in a form either 1) (Posynomial) < (Affine) or 2) Posynomial inequalities.

Note that $\alpha_i \sqrt[3]{v_i(k\Delta t)} + \beta_i \sqrt{v_i(k\Delta t)} + \gamma_i v_i(k\Delta t) + \delta_i$ is posynomial because all the $\alpha_i, \beta_i, \gamma_i$ and δ_i are positive, and measured vibration is always positive. Therefore, since the class of posynomial is closed under summation, all the constraints on the left hand side are posynomial.

We can now solve Equation 16 very efficiently, roughly proportional to $\max\{n^3, n^2 m, F\}$, where n is the number of variables, m the number of constraints, and F is the cost of evaluating a posynomial's first and second derivative. Additionally, we can guarantee a global optimum since it is a mixed linear GP problem. Note that GPs are a special class of mathematical programs that can be converted to convex form using a change of variable. However, CVX [22] performs well on medium-scale GP problems, and it is thus not necessary to perform this intermediate step.

Solving Equation 16 provides us with vibration propagation coefficients and flow rate parameters, but its performance may be affected due to relaxed constraints. Therefore, we also introduce a two phase LP problem which can solve the same set of equations.

4.6 Two Phase Linear Programming Model

We reduce the complexity of solving Equation 11 by deriving it as an approximate LP problem. The propagation coefficients are unknown and need to be estimated. However, since pipe topology is static and not expected to change significantly over time, we can estimate the propagation coefficients opportunistically. After computing these coefficients, Equation 11 becomes a LP problem because the posynomial equality terms become linear equations. Therefore, the problem can be decomposed into two problems: (a) vibration propagation coefficient estimation, and (b) water flow rate parameter estimation.

4.6.1 Vibration Propagation Parameter Estimation

It is likely that only one pipe j has running water during some period, and thus the system can measure the vibration propagation between the pipes. In this case, $\tilde{v}_j = v_j$. The measured vibration on every other pipe i can then be estimated by

$$
\tilde{v}_i = p_{i,j} \tilde{v}_j. \qquad (17)
$$

Additionally, the following holds true:

$$
\begin{aligned}
p_{i,j} &= \; 1 \text{ if } i = j \\
p_{i,j} &= \; \frac{\tilde{v}_i}{\tilde{v}_j} \text{ otherwise} \qquad (18)
\end{aligned}
$$

If the system behaved ideally, the measurements would be perfect, and the propagation coefficient computation would be trivial. However, inherent measurement noise requires us to reformulate this as a parameter estimation problem. We choose L1-norm minimization with linear inequality constraints, since this tends to be less sensitive to significant outliers compared to a least squares approach. According to previously published results in sensor networks [11,23,24,27], inexpensive sensors on motes tend to have significant outliers and faults.

The problem is solvable using a standard LP solver with the appropriate linear inequality constraints. We define l as the sample index, and let L be the total number of samples. The problem is then,

$$
\begin{aligned}
\min \quad & \left\lVert \tilde{\mathbf{V}}_i - p_{i,j} \tilde{\mathbf{V}}_j \right\rVert_1 \\
\text{subject to} \quad & \begin{array}{ll} p_{i,j} = 1 & \text{if } i = j \\ 0 \le p_{i,j} < 1 & \text{else} \end{array} \qquad (19)
\end{aligned}
$$

where,
$$\tilde{\mathbf{V}}_i = [\tilde{v}_i(1), \tilde{v}_i(2), ..., \tilde{v}_i(L)]^T \in \mathbb{R}_+^L$$
$$\tilde{\mathbf{V}}_j = [\tilde{v}_j(1), \tilde{v}_j(2), ..., \tilde{v}_j(L)]^T \in \mathbb{R}_+^L$$

4.6.2 Vibration to Water Flow Rate Parameter Estimation

Once we compute the vibration propagation coefficients, the problem simplifies to a standard LP problem since the matrix $\mathbf{P} = [p_{i,j}]$ is now known and invertible. Finally, we solve

$$\begin{aligned} \min \quad & ||\mathbf{M} - \mathbf{F}||_1 \\ \text{subject to} \quad & 0 \leq f_i(k\Delta t) \leq f_{i,max} \\ & \mathbf{V}(k\Delta t) = \mathbf{P}^{-1}\tilde{\mathbf{V}}(k\Delta t) \end{aligned} \quad (20)$$

where
$$k = 1, 2, ..., K$$
$$\mathbf{P} = [p_{i,j}]$$
$$\mathbf{V}(k\Delta t) = [v_1(k\Delta t), v_2(k\Delta t), ..., v_N(k\Delta t)]^T \in \mathbb{R}_+^N$$
$$\tilde{\mathbf{V}}(k\Delta t) = [\tilde{v}_1(k\Delta t), \tilde{v}_2(k\Delta t), ..., \tilde{v}_N(k\Delta t)]^T \in \mathbb{R}_+^N$$

4.7 Correction Mechanism and Performance Metric

Solving the optimization problem above, the system can estimate the parameters required to map vibration measurements to flow rate. However, system characteristics can change over time due to topological changes, seasonal temperature variations and aging. Therefore, we need a mechanism that tests the system performance and recalibrates the mapping, if necessary, through iteratively solving the optimization problems.

We define a performance metric

$$\text{Performance} \overset{def}{=} \left| \frac{\sum_{i=1}^{N} \hat{f}_i(t) - M(t)}{M(t)} \right| \quad (21)$$

where, $\hat{f}_i(t)$ is the estimated flow rate in pipe i. If its value is close to 0, we know the system is performing well, since the sum of the estimated flow rates has to be close to the total flow rate $M(t)$. However, if the metric exceeds a set threshold ϵ, the system needs recalibration.

A further improvement can be made based on this observation. By normalizing each estimated flow rate $\hat{f}_i$ with the ratio of the total flow rate to the sum of all estimated flow rates, i.e.,

$$\tilde{f}_i(t) = \frac{\hat{f}_i(t)M(t)}{\sum_{i=1}^{N} \hat{f}_i(t)} \quad (22)$$

we ensure that $\sum_{i=1}^{N} \tilde{f}_i = M(t)$ and is nearer the real flow rate in the pipe.

5. SYSTEM DESCRIPTION

A user installs the vibration sensors on the pipes in their plumbing and specifies the topology to formulate the optimization problem. Thereafter, the system runs autonomously. First, it collects vibration and water flow rate data to get a solution to the optimization problem. After the parameters are found, the system can estimate the individual flow rate in each pipe. Simultaneously, the system calculates and tests the performance metric introduced in Section 4.7. If
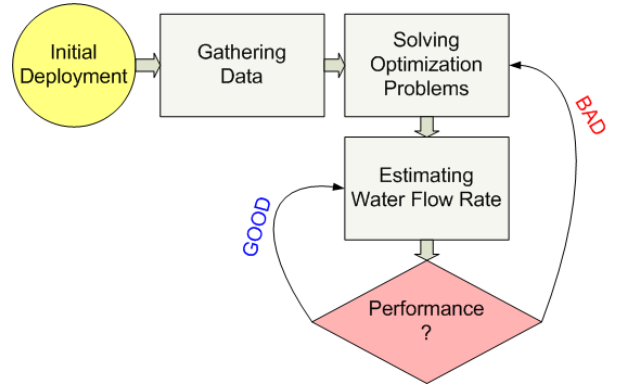

Figure 7: Algorithm flowchart for NAWMS. After an initial data gathering, NAWMS solves an optimization problem to retrieve the calibration parameters. During system runtime, NAWMS monitors its own performance. If the performance is bad, it recalibrates itself.

Table 1: Pipe Properties

Pipe Number	Pipe Material	Diameter
Pipe 1	Copper	3/4 in (19.05mm)
Pipe 2	PVC	3/4 in (19.05mm)
Pipe 3	PVC	1 in (25.4mm)

this metric exceeds a user specified threshold ϵ, the system recalibrates and solves the optimization problem again. Figure 7 illustrates this algorithm in a flow chart.

6. EVALUATION

In order to test and validate our system, we constructed a plumbing testbed with three pipes of different materials and diameters. Table 1 summarizes the pipe properties, and Figure 8 shows a picture of the setup. The main water pipe is equipped with a commercial water flow meter that generates a pulse train proportional to the flow rate. We connected this pulse train to a Crossbow MicaZ mote that provides the fusion center with real-time flow rate measurements $M(t)$.

Each branch of the testbed is equipped with an accelerometer. In our setup, we use a MicaZ mote with the MTS310 sensor board. The MTS310 sensor board contains a 2D Analog Device ADXL202 accelerometer that has a range of $\pm 2g$. The node samples the axis perpendicular to the pipe at 100Hz and calculates the variance of acceleration every 50 samples. This variance, $\tilde{v}_i(k\Delta t)$, is then sent to the fusion center for further processing.

In addition to the sensors, each branch has a ball type valve at the end in order to control the flow rate within each pipe. To get the per-pipe ground truth, we added another flow rate meter to the end of each pipe.

6.1 Evaluation of Water Flow Rate Model

6.1.1 Vibration to Water Flow Rate Model Validation

Equation (3) suggests that the relation between the vibration variance and the flow rate is linear. Unfortunately, because of modeling inaccuracy and sensor characteristics, the relationship is non-linear as Figures 3 and 4 suggest. Using a good fitting model is essential in order to minimize the

Table 2: Vibration to Water Flow Rate Fitting Model

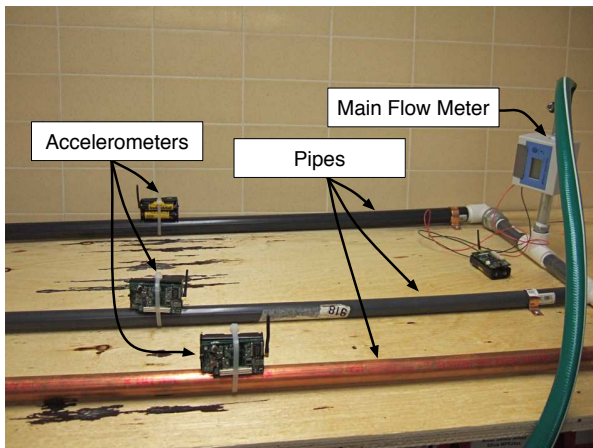| Pipe	Fitting Model	Coefficient	Fitting Error
Copper Pipe	$f(t) = \alpha \sqrt[3]{v(t)} + \beta \sqrt{v(t)} + \gamma v(t) + \delta$	$\alpha = 0.1548, \beta = 0, \gamma = 0, \delta = 0.0472$	1.865
	$f(t) = \beta \sqrt{v(t)} + \gamma v(t) + \delta$	$\beta = 0.1067, \gamma = 0, \delta = 0.0923$	2.030
	$f(t) = \gamma v(t) + \delta$	$\gamma = 0.0478, \delta = 0.1470$	2.724
PVC Pipe	$f(t) = \alpha \sqrt[3]{v(t)} + \beta \sqrt{v(t)} + \gamma v(t) + \delta$	$\alpha = 0.0896, \beta = 0, \gamma = 0, \delta = 0.0160$	1.058
	$f(t) = \beta \sqrt{v(t)} + \gamma v(t) + \delta$	$\beta = 0.0530, \gamma = 0, \delta = 0.0520$	1.282
	$f(t) = \gamma v(t) + \delta$	$\gamma = 0.0154, \delta = 0.0884$	1.892

Figure 8: Image of the plumbing testbed showing the three pipes with accelerometers, and the main water flow meter.

Figure 9: Vibration induced by water flow in pipe 2 propagates to pipe 1 and 3. NAWMS has to compensate for this effect to minimize estimation error.

Figure 10: Water flow rate estimate for a single pipe.

estimation error. A commonly used fitting model would be a polynomial function. But our prior measurements showed the vibration in a pipe saturates at some point. This effect is better captured with a square root, or even 3rd order root curve. Table 2 summarizes the different fitting curves, their parameters, and the fitting error for two different types of pipe material. We see that a 3rd order root curve has the least fitting error for both pipes. Higher order root curves might fit better, but the increase in complexity (more calibration parameters to estimate) does not ratify the small gain in fitting error.

6.1.2 Vibration Propagation Among Pipes

To verify the vibration propagation among the pipes, we turned on one pipe, and measured the vibration occurring on all three pipes. Figure 9 depicts the case where pipe 2 is running, and we plot the vibration of pipe 2 versus the vibration of pipe 1 and 3. We see that our first order approximation in Equation 10 is reasonable and yields a good fit on the collected data, though the variation within the samples is very large. This might limit the achievable precision in the flow estimation, but we illustrate in the next section how this can be ameliorated. Future research on this could further improve the propagation model by accounting for vibration propagation time.

6.2 Flow Rate Estimation

For all of the following experiments, we used the two phase LP problem to get the calibration information. In the first experiment, we investigate how well the system can track the flow in only one pipe. Thus, the flow rate in the main pipe
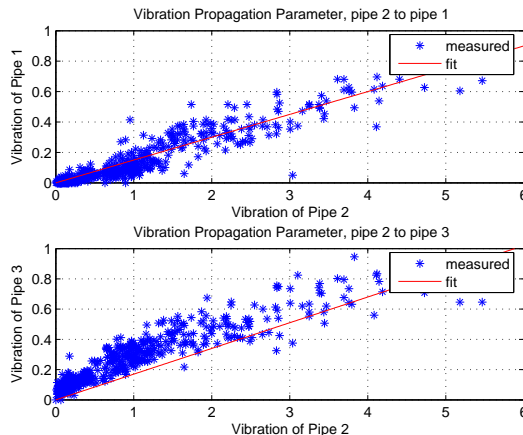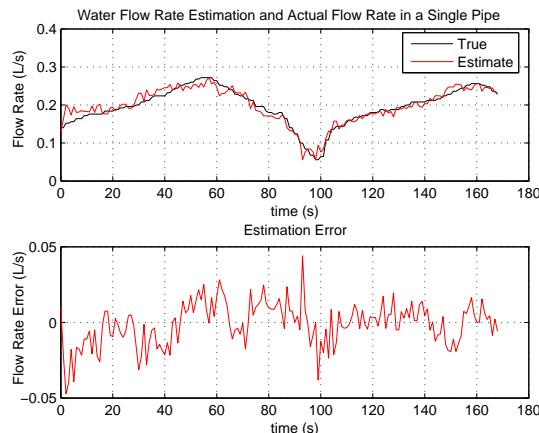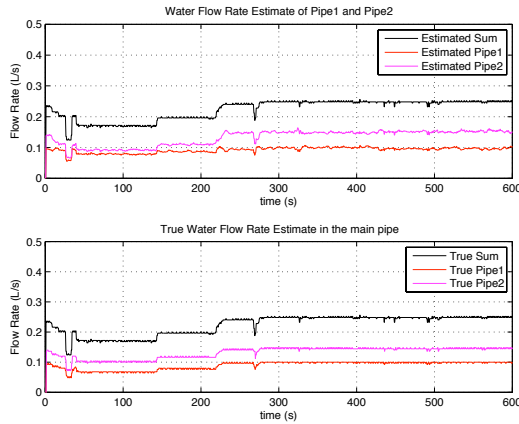
Figure 11: Water flow rate estimation of pipe 1 and 2. The top graph shows NAWMS estimated flow, the bottom is the ground truth measured by the per pipe flow meters.
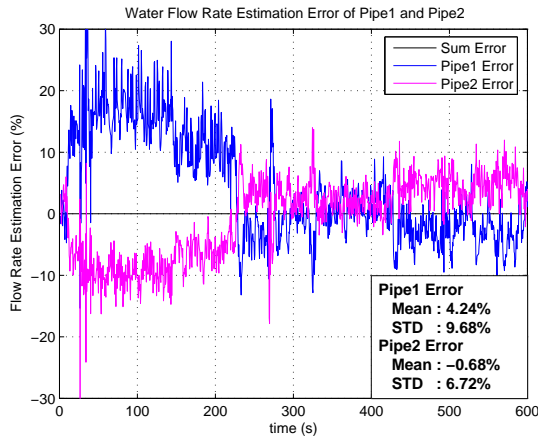

Figure 12: Water flow rate estimation error for pipe 1 and 2. The flow estimation is higher at low absolute flow rates ($t = [0, 230]$ seconds) because of resolution problems in the ADC.

was the same as the flow rate in the pipe under investigation. Figure 10 shows the result. On average, the estimation error over the 180 second experiment was -0.49%, with a standard deviation of 9.93 (In absolute numbers mean -0.0049L/s with a standard deviation of 0.014).

We now focus on the concurrent estimation of the flow rate in two pipes. Figure 11 compares the ground truth measurements (lower graph) to the estimated flow rate within the pipes and Figure 12 depicts its relative error. We see that the error of the sum of the two estimated flows is almost 0. This is not surprising given that we normalize the two individual flows with the sum. Note that the relative error reduces after about 230 seconds. The reason for this is that the actual water flow rate almost doubled after that point. While the accelerometer has enough sensitivity for low vibrations, our current 10 bit ADC lacks the necessary resolution to get below 0.004g, and thus a higher error at lower flow rates is to be expected. Our next prototype will take care of this by providing a signal amplifier in these low
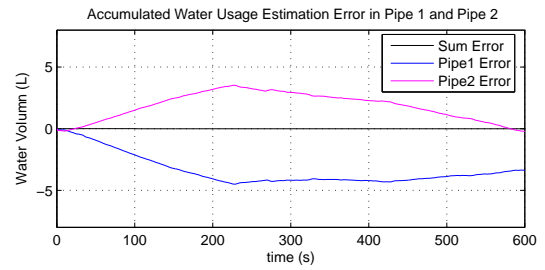

Figure 13: Accumulated water usage estimation error. The total water used was approximately $400L$.
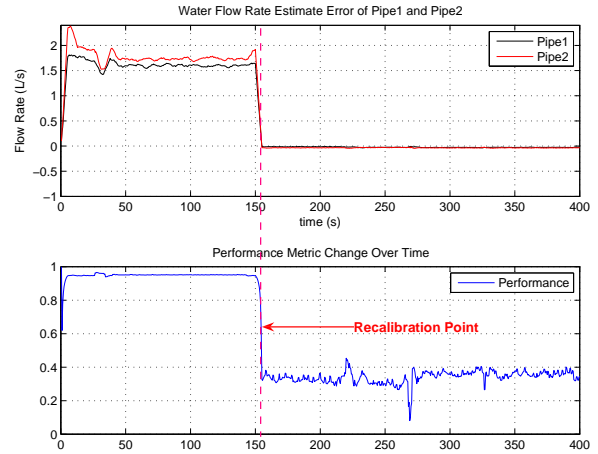

Figure 14: After an initial guess of the calibration parameters, NAWMS recalibrates at $t = 150$ and the performance metric improves considerably.

vibration regions. Figure 13 shows the error in the accumulated per pipe water usage and we see that it stays low, even over a long period of time and high volume of water.

It is interesting to see how well our different modeling parameters influence the estimation accuracy. For this purpose, we ran the different optimization calculations from Section 4 on the same experimental data. A summary of the result can be found in table 3. In the first calculation, we didn't use any compensation (Figure 15a) and thus the estimation doesn't account for vibration propagation, nor uses the normalization correction. In the second calculation, we accounted for vibration propagation only (Figure 15b). We see that just accounting for this improves the estimation by more than a factor of 2. In the third calculation, we used the normalization correction described in Section 4.7 (Figure 15c). The effect on the precision of the estimation is tremendous, since now the error of the sum of the two vibration estimates is forced to be 0. Last, using all the correction mechanisms and accounting for vibration propagation and normalizing the two flows yields the best result (Figure 15d). This shows that our modeling of vibration effects and correction mechanisms are efficient and help reducing the overall estimation error.

Our last experiment shows the effectiveness of the performance metric. Figure 14 depicts the experiment result. First, we assumed some wrong calibration parameters and
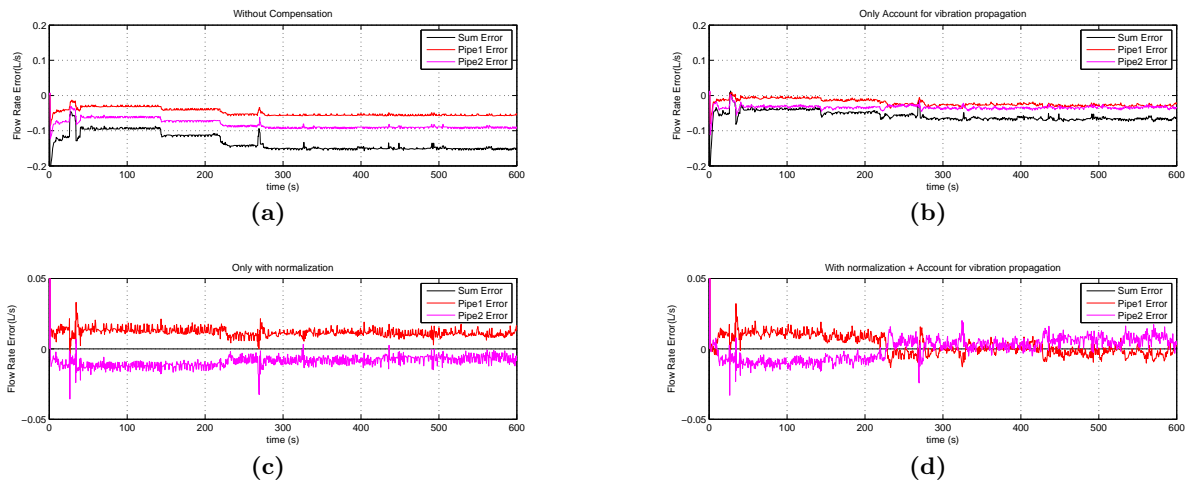
Figure 15: Adding the different water flow models and compensation techniques increases the precision of the water flow estimation. (a) is the baseline where no additional compensations are made. (b) accounts for vibration propagation. (c) normalizes the individual flow rates with the total flow rate in the main pipe, and (d) shows NAWMS' performance while accounting for vibration propagation and normalizing the individual flow rates.

Table 3: Estimation improvement by using different flow rate models and compensation techniques

Scheme	Pipe 1		Pipe 2	
	Mean Error	STD	Mean Error	STD
None	-0.054L/s (-53.1%)	0.011	-0.094L/s (-63.0%)	0.017
Vib Prop	-0.016L/s (-15.8%)	0.010	-0.040L/s (-26.8%)	0.009
Normalization	0.016L/s (15.6%)	0.006	-0.013L/s (-8.5%)	0.006
Both	0.010L/s (9.6%)	0.010	-0.007L/s (-4.4%)	0.011

used them to calculate the estimated flow rate. At $t = 150$ seconds, the algorithm decides to recalibrate the system, using the data collected between $t = [0, 150]$. The water flow rate estimation error after that point immediately drops to almost 0, and the performance metric goes from almost 1 down to approximately 0.4. This shows that using this performance metric, an efficient recalibration scheme can be developed and used to keep the system accurate and efficient.

7. FUTURE WORK

Our testbed shows that it is feasible to exploit the correlation among vibration on each of pipes and the main meter reading to estimate water flow rate in individual pipe.

One limitation of the current system architecture is the requirement of having a sensor on each pipe. This can quickly become tedious and cost intensive as the pipes have to be exposed in order to install a sensor on them, and as the size of the pipe topology increases. In a typical household, however, the number of water faucets is limited. For example, a bathroom usually has 5-7 water outlets, a kitchen has 4 water pipes for a sink and a dishwasher, and a laundry room has 3-4 water outlets. From a simple calculation, a 3-bed and 2-bathroom house has approximately 17-21 outlets excluding outlets for the outdoor purpose. This basically means that we need around 20 vibration sensors to estimate water flow rate.

In a building, however, the number of pipes is much more than this. To cope with this problem, we are currently exploring ways of estimating the water flow rate with a fewer amount of sensors. One possibility exploits the vibration propagation within the pipes. By detecting a specific signature of propagated vibration, it might be possible to estimate the flow in pipes that do not have a sensor on them.

Since the vibration is mechanically propagating, pipes, physically mounted on a wall, are sensitive to external vibration sources. Although our testbed showed that it is quite robust to the external vibration sources such as foot steps, hitting the wall, and other typical activities in a room, a real house deployment can reveal interesting research questions about how to cope with external noise sources to get a better estimate.

With a slight modification, we envision that our proposed framework for water monitoring could be applied to other resource monitoring systems. For example, the electric energy distribution in a household has a very similar architecture to the water monitoring system. It has one main meter, and there exist simple to install sensors that need to be calibrated in order to estimate the power consumption of an appliance [26]. The same is true for natural gas for heating and cooking.

A further application of our system would be activity classification, since water usage inherently requires human presence, similar to [21]. However, the information that the system would provide could be more meaningful since it could help people improve their natural resource efficiency.

Lastly, but not least, we want to investigate how a leak will affect the overall system's performance and how we can detect the leak. If a leak suddenly happens, one can imagine that the vibration to water flow rate parameters change thus

the estimation error will become worse. The main question is to find out how the parameters change or what other signatures we need to have. Once this is done, the system could further alarm the owner if it detects that an unusual amount of water, or a continuous amount of water suggesting a leak or criminal activity. This can be especially helpful for outdoor irrigation systems where the owner might not be able to immediately detect a water leak, because the visible effects disappear quickly.

8. CONCLUSION

We have introduced a less intrusive, auto-calibrated, per pipe water monitoring system that provides spatially fine grained real-time water usage previously not possible without extensive installation of inline sensors. In our work, we considered various pipe topologies and formulated several optimization problems that yield the system calibration coefficients. The system makes extensive use of a two-tired architecture and exploits pre-installed equipment that can usually be found in a household.

In our experimental results, we showed that vibration based water flow rate estimation is feasible and that the achieved individual per pipe flow rate error on average is less than 10%. By introducing a performance metric, we can efficiently monitor the system calibration status, and automatically decide if recalibration is necessary.

9. ACKNOWLEDGMENTS

10. REFERENCES

[1] AMERICAN WATER WORKS ASSOCIATION. C706-96(r05) : Awwa standard for direct-reading remote-registration systems for cold-water meters. *STC* (2005).

[2] AUTOMATIC METER READING ASSOCIATION. http://www.amra-intl.org/.

[3] BANKSTON, JR., J., AND BAKER, F. E. Open channel flow in aquaculture. *SRAC Publication No.374* (1995).

[4] BIRD, R. B., STEWART, W. E., AND LIGHTFOOT, E. N. Transport phenomena. *John Wiley and Sons Inc., NY, pp. 153 179, Chap. 5* (1960).

[5] BLAKE, W. K. *Mechanics of Flow-Induced Sound and Vibration.* Academic Press Inc., Harcort Brace Jovanokich Publishers, Orlando, 1986.

[6] BOYD, S., AND VANDENBERGHE, L. Lecture notes on convex optimization. http://www.stanford.edu/class/ee364a/lectures.html.

[7] BOYD, S., AND VANDENBERGHE, L. *Convex Optimization.* Cambridge University Press, 2004.

[8] BOYD, S. P., KIM, S. J., VANDENBERGHE, L., AND HASSIBI, A. A tutorial on geometric programming. http://www.stanford.edu/ boyd/papers/gp_tutorial.html, 2005.

[9] CANTONI, M., WEYER, E., LI, Y., OOI, S., MAREELS, I., AND RYAN, M. Control of large-scale irrigation networks. *Proceedings of IEEE Vol. 95, No. 1* (January 2007).

[10] CENTER FOR ECOLOGY & HYDROLOGY. The water poverty index. http://www.ceh.ac.uk/sections/ph/WaterPovertyIndex.html, 2005.

[11] CHEN, J., KHER, S., AND SOMANI, A. Distributed fault detection of wireless sensor networks. *International Conference on Mobile Computing and Networking, ACM* (2006).

[12] CHEUNG, E. Municipal water meter monitor. http://www.edcheung.com/automa/water.htm, 2005.

[13] CHIANG, M. Geometric programming for communication systems. *now Publishers Inc* (2005).

[14] DAHL, J., AND VANDENBERGHE, L. Cvxopt. http://abel.ee.ucla.edu/cvxopt.

[15] DEVICES, E. E. Watts up? pro. http://www.wattsupmeters.com/.

[16] DYNASONICS. Ultrasonic water flow meters. http://www.dynasonics.com/.

[17] ENBW ENERGIE BADEN-WÜRTTEMBERG AG. Der intelligente stromzähler. http://www.enbw.com/.

[18] ESTER, P. *Consumer Behavior and Energy Conservation: A Policy-Oriented Experimental Field Study on the Effectiveness of Behavioral Interventions Promoting Residential Energy Conservation.* Boston: Martinus Nijhoff Publishers, 1985.

[19] EUROPEAN PATENT. Ultrasonic flow meter, flow measurement method, and computer program. *EP1887327* (2006).

[20] EVANS, R. P., BLOTTER, J. D., AND G. STEPHENS, A. Flow rate measurements using flow-induced pipe vibration. *Transactions on the ASME 126* (2004), 280.

[21] FOGARTY, J., AU, C., AND HUDSON, S. E. Sensing from the basement: A feasibility study of unobtrusive and low-cost home activity recognition. *ACM UIST* (2006).

[22] GRANT, M., BOYD, S., AND YE, Y. Cvx: Matlab software for disciplined convex programming. http://www.stanford.edu/ boyd/cvx/, March 2008.

[23] GUPTA, G., AND YOUNIS, M. Fault-tolerant clustering of wireless sensor networks. *Wireless Communications and Networking, 2003. WCNC 2003. 2003 IEEE 3* (16-20 March 2003), 1579–1584 vol.3.

[24] HUANG, Y., LUO, X., AND DONG, M. On distributed fault-tolerant detection in wireless sensor networks. *IEEE Trans. Comput. 55, 1* (2006), 58–70.

[25] KENT/AMCO. Industrial pulsers for c700. http://jerman.com/kmmeters.html.

[26] LELAND, E. S., WHITE, R. M., AND WRIGHT, P. K. Energy scavenging power sources for household electrical monitoring. *PowerMEMS* (Dec. 2006).

[27] LYMBEROPOULOS, D., LINDSEY, Q., AND SAVVIDES, A. An empirical analysis of radio signal strength variability in ieee 802.15.4 networks using monopole antennas. *ENALAB Technical Report 050501* (2006).

[28] MCMAKIN, A. H., MALONE, E. L., AND LUNDGREN, R. E. Motivating residents to conserve energy without financial incentives. *Environment and Behavior Journal* (2002).

[29] MOSEK INC. The mosek optimization software. http://www.mosek.com.

[30] PAEK, J., CHINTALAPUDI, K., GOVINDAN, R., CAFFREY, J., AND MASRI, S. A wireless sensor network for structural health monitoring: Performance and experience. *Workshop on Embedded Networked Sensors, ACM* (2005).

[31] PATEL, S. N., ROBERTSON, T., KIENTZ, J. A., REYNOLDS, M. S., AND ABOWD, G. D. At the flick of a switch: Detecting and classifying unique electrical events on the residential power line. *Ubicomp,* (2007).

[32] PITTARD, M. T., AND BLOTTER, J. B. Numerical modeling of les based turbulent-flow induced vibration. *ASME International Mechanical Engineering Congress & Exposition* (2003).

[33] PRASHUN, A. L. Fundamentals of fluid mechanics. *Prentice Hall, Englewood Cliffs, NJ, pp. 202 222, Chap. 7.* (1980).

[34] SETO, W. W. *Theory and Problems of Mechanical Vibrations.* SchaumPublishing Co., NY, pp. 128, Chap. 5., 1964.

[35] SMARTMETER. http://www.smartmeter.co.uk/.

[36] SONMEZ, F. K., APAYDIN, H., OZTURK, A., AND KODAL, S. Open canal irrigation network optimization: a case study for burdur-turkey. *Pakistan Journal of Biological Sciences 8* (2005), 1064–1073.

[37] SRITHARAN, S. S. *Optimal Control of Viscous Flow.* SIAM, 1998.

[38] STERN, P. C. Information, incentives, and proenvironmental consumer behavior. *Journal of Consumer Policy* (1999).

[39] STOIANOV, I., NACHMAN, L., MADDEN, S., AND TOKMOULINE, T. Pipeneta wireless sensor network for pipeline monitoring. *IPSN* (2007), 264–273.

[40] TRIMMER, W. L. Estimating water flow rates. *Oregon State University Extension Service* (1994).

[41] U. S. ENVIRONMENTAL PROTECTION AGENCY. Watersense. http://epa.gov/watersense/index.htm.